



A multi-wavelength study of the unidentified TeV γ -ray source HESS J1626–490

P. EGER¹, G. ROWELL², A. KAWAMURA³, Y. FUKUI³, L. ROLLAND⁴, C. STEGMANN¹

¹*Erlangen Centre for Astroparticle Physics, Universität Erlangen-Nürnberg, Erwin-Rommel-Str. 1, 91058 Erlangen, Germany*

²*School of Chemistry and Physics, University of Adelaide, Adelaide 5005, Australia*

³*Department of Astrophysics, Nagoya University, Furocho, Chikusaku, Nagoya 464-8602, Japan*

⁴*CEA Saclay, DSM/IRFU, F-91191 Gif-Sur-Yvette Cedex, France; now at Laboratoire d'Annecy-le-Vieux de Physique des Particules (LAPP), Université de Savoie, CNRS/IN2P3, F-74941 Annecy-Le-Vieux, France*

peter.eger@physik.uni-erlangen.de

DOI: 10.7529/ICRC2011/V07/0035

Abstract: HESS J1626–490, so far only detected with the H.E.S.S. array of imaging atmospheric Cherenkov telescopes, could not be unambiguously identified with any source seen at lower energies.

Therefore, we analyzed data from an archival *XMM-Newton* observation, pointed towards HESS J1626–490, to classify detected point-like and extended X-ray sources according to their spectral properties. None of the detected X-ray point sources fulfills the energetic requirements to be considered as the synchrotron radiation (SR) counterpart to the VHE source assuming an Inverse Compton (IC) emission scenario. Furthermore, we did not detect any diffuse X-ray excess emission originating from the region around HESS J1626–490 above the Galactic Background. The derived upper limit for the total X-ray flux disfavors a purely leptonic emission scenario for HESS J1626–490.

To characterize the Interstellar Medium surrounding HESS J1626–490 we analyzed ¹²CO(J=1-0) molecular line data from the NANTEN Galactic plane survey and HI data from the Southern Galactic Plane Survey (SGPS). We found a good morphological match between molecular and atomic gas in the –27 km/s to –18 km/s line-of-sight velocity range and HESS J1626–490. The cloud has a mass of $1.8 \times 4 M_{\odot}$ and is located at a mean kinematic distance of $d = 1.8$ kpc. Furthermore, we found a density depression in the HI gas at a similar distance which is spatially consistent with the SNR G335.2+00.1.

Therefore, the most likely origin of the VHE γ -ray emission observed with H.E.S.S. is the hadronic interaction of cosmic rays with a moderately dense molecular cloud, which we detected with *Nanten*. The application of a detailed hadronic model for cosmic ray transport and interaction shows that the cosmic rays could originate from the nearby SNR G335.2+00.1.

Keywords: acceleration of particles, ISM: supernova remnants, ISM: clouds, ISM: individual objects: HESS J1626–490, X-rays: ISM, submillimeter: ISM

1 Introduction

HESS J1626–490 is a VHE γ -ray source of unknown origin, which so far could not be identified with any counterpart at lower wavelengths. This object, with an intrinsic extension of ~ 5 arcmin (Gaussian FWHM), is located right on the Galactic plane (R.A.: $16^{\text{h}}26^{\text{m}}04^{\text{s}}$, Dec.: $-49^{\circ}05'13''$) and was detected by H.E.S.S. with a peak significance of 7.5σ [1]. These authors measured a power-law spectrum with a photon index of $2.2 \pm 0.1_{\text{stat}} \pm 0.2_{\text{sys}}$ and a flux normalization of $(4.9 \pm 0.9) \times 10^{-12} \text{cm}^{-2} \text{s}^{-1} \text{TeV}^{-1}$ at 1 TeV at energies between 0.5 TeV and 40 TeV.

In this work we analyzed the data of an archival *XMM-Newton* observation to search for an X-ray counterpart to HESS J1626–490. Therefore, we classified the detected X-

ray point sources in the vicinity of HESS J1626–490 and searched for possible diffuse excess emissions above the expected Galactic background. Furthermore, we present ¹²CO(J=1-0) molecular line survey data taken with the *Nanten* mm/sub-mm observatory to scan for molecular clouds, and SGPS HI data to characterize the neutral interstellar medium.

2 XMM-Newton X-ray data analysis and results

We analyzed the EPIC-pn and MOS data of an archival *XMM-Newton* dataset (ID: 0403280201) pointed towards the direction of HESS J1626–490. After screening for pe-

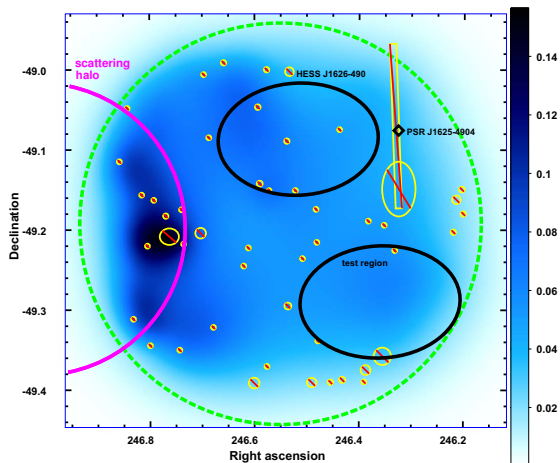


Figure 1: Adaptively smoothed EPIC-PN image of diffuse X-ray flux in the 3–7 keV energy band with a linear color scale (arbitrary units). The instrument FoV is shown as a dashed circle (green). The large ellipses (black) denote the extraction regions for HESS J1626–490 and the background test, respectively. The large circle (magenta) to the east gives the approximate extension of the X-ray scattering halo of 4U 1624-490. Excluded regions are shown as crossed-out areas (yellow regions crossed with red lines)

riods of enhanced background activity the net exposures for pn and MOS are 4.9 ks and 13.2 ks, respectively.

Using the standard maximum likelihood technique of the Science Analysis Software (SAS) we searched for X-ray point sources within the 4σ VHE γ -ray contours of HESS J1626–490. Twelve such sources were detected in this region above a limiting flux of $\sim 2 \times 10^{-14}$ erg cm $^{-2}$ s $^{-1}$. We characterized these sources according to their X-ray spectral properties as well as their near-infrared counterpart from the 2MASS all-sky catalog [2]. Based on this classification scheme (for more details see [3]) we calculated the unabsorbed fluxes for all detected point sources, assuming different spectral shapes and foreground hydrogen column densities, depending on the source class. By far the brightest detected X-ray source features a soft thermal X-ray spectrum with an unabsorbed flux of 7.9×10^{-12} erg cm $^{-2}$ s $^{-1}$ (0.5 – 10 keV), and can be identified with a triplet system of coronally active main sequence stars. All other X-ray sources feature unabsorbed fluxes $< 3.5 \times 10^{-13}$ erg cm $^{-2}$ s $^{-1}$ (0.5 – 10 keV).

We also searched for a potential extended and diffuse X-ray component related to HESS J1626–490. [1] approximated the morphology of HESS J1626–490 by fitting a 2-D Gaussian to the VHE γ -ray excess map. The resulting intrinsic (with the effects of the instrument point-spread-function removed) major and minor axes are 0.1° and 0.07° , respectively, with a position angle of 3° west to north. From the same region we searched for diffuse and extended X-ray emission above the astrophysical and instrumental background components. Figure 1 shows a

smoothed image of the diffuse X-ray flux in the 3–10 keV band. Point-like sources were removed, based on the 99% energy containment radius of the PSF. Also, the read-out streak caused by the brightest source in the FoV has been excluded. The instrumental and particle-induced background components were subtracted using a non-X-ray background dataset from the calibration database. Apart from some contamination towards the east of the FoV due to an X-ray scattering halo caused by the bright binary system 4U 1624-490, the level of diffuse X-ray emission appears to be homogeneous and flat throughout the FoV. To quantify potential diffuse excess X-ray emission from the direction of HESS J1626–490 and to compare the signal to the expected diffuse Galactic background, we extracted a spectrum from an elliptical region compatible with the intrinsic VHE γ -ray extent, as well as from a test region in the southern part of the *XMM-Newton* FoV (as indicated in Fig. 1). We found no indication for enhanced X-ray emission from HESS J1626–490 compared to the test region, and the spectra from both regions are compatible with typical diffuse Galactic X-ray emission expected from such a region in the Galactic plane (see, e.g., [4]). We derived an upper limit for extended X-ray emission connected to HESS J1626–490 of $F_{X,\text{excess}} < 4.9 \times 10^{-12}$ erg cm $^{-2}$ s $^{-1}$ (1–10 keV), assuming a powerlaw spectral shape with index -2 .

3 *Nanten* $^{12}\text{CO}(J=1-0)$ and SGPS HI data

To search for molecular clouds, spatially and morphologically coincident with HESS J1626–490, we analyzed $^{12}\text{CO}(J=1-0)$ molecular line observations performed by the 4 m mm/sub-mm *Nanten* telescope, located at Las Campanas Observatory, Chile [5]. For this work the local standard of rest velocity (v_{LSR}) range -240 to $+100$ km s $^{-1}$ was searched.

Figure 2 shows the *Nanten* $^{12}\text{CO}(J=1-0)$ image integrated over the v_{LSR} range -31 to -18 km s $^{-1}$. In this interval we found a ^{12}CO feature partially overlapping with the VHE emission. According to the Galactic rotational model of [6], this v_{LSR} range corresponds to a kinematic distance of 1.5 to 2.2 kpc. Using the relation between the hydrogen column density (N_{H}) and the $^{12}\text{CO}(J=1-0)$ intensity $W(^{12}\text{CO})$, $N_{\text{H}} = 1.5 \times 10^{20}$ [W(^{12}CO)/K km/s] [7], we estimate the total mass of this cloud at $1.8 \times 10^4 M_{\odot}$ for $d = 1.8$ kpc within an elliptical region centered at $l = 334.78$, $b = 0.00$ with dimensions 0.26×0.30 deg. The corresponding average density is 2.1×10^2 cm $^{-3}$.

In addition to the *Nanten* ^{12}CO molecular line data which trace the densest regions of the interstellar gas, we also investigated the environment of HESS J1626–490 using HI data from the Southern Galactic Plane Survey (SGPS). Figure 3 shows the v_{LSR} profile for this region integrated over the Galactic latitude range -0.11 to 0.24 deg, which is also the extent of the VHE γ -ray signal of HESS J1626–490. This image shows a region of increased gas density in spatial coincidence with the CO molecular cloud, most pro-

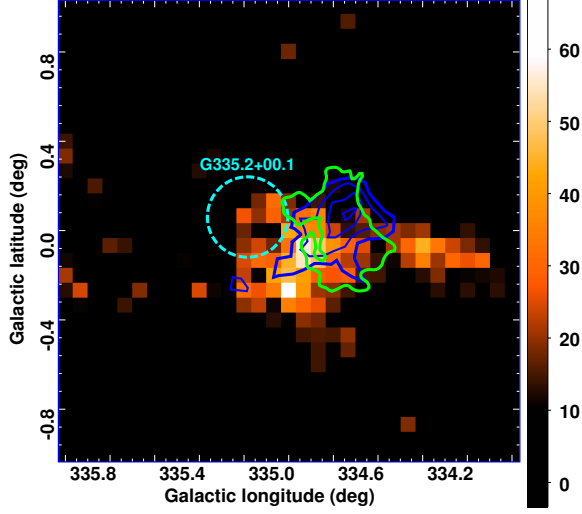


Figure 2: *Nanten* $^{12}\text{CO}(J=1-0)$ image of the region around HESS J1626–490 (linear scale in K km s^{-1}) integrated over the v_{LSR} range -31 to -18 km s^{-1} . Overlaid are the contours of the VHE emission (blue) and of the HI cloud discussed in Sect. 3 (green). The dashed circle (light blue) denotes the position and extension of SNR G335.2+00.1.

nounced in the -31 to -23 km s^{-1} velocity range. The contours extracted from an HI image integrated over this velocity range are shown in Fig. 2. We estimated the mass of the dense HI region coinciding with the VHE and ^{12}CO features using the signal within the same elliptical region as for the CO cloud (Sect. 3). Using the relation between HI intensity and column density from [8] ($X=1.8 \times 10^{18} \text{ cm}^{-2} \text{ K}^{-1} \text{ km/s}$) we estimated the mass of the cloud as $4.9 \times 10^3 M_{\odot}$ with an average density of 60.1 cm^{-3} . Furthermore, a local HI density depression is seen in the center of the image at an angular separation of $\sim 21'$ from the CO molecular cloud and HESS J1626–490. It is striking that this feature is consistent in position as well as in angular extension with the SNR G335.2+00.1 [9, 10].

4 Discussion

In this section we discuss potential emission scenarios giving rise to the VHE γ -ray signal detected with H.E.S.S., particularly in the context of the presented multi-wavelength data.

In the case of a leptonic scenario where low-energy photons are up-scattered by relativistic electrons via the IC process, X-ray emission is expected to accompany the VHE γ -ray signal arising from synchrotron cooling of the same population of high-energy electrons [11]. Even from a first glance at the flux levels in X-rays ($\sim 10^{-13} \text{ erg cm}^{-2} \text{ s}^{-1}$ for point sources and $\sim 10^{-12} \text{ erg cm}^{-2} \text{ s}^{-1}$ for diffuse emission) and at VHE γ -rays ($\sim 10^{-11} \text{ erg cm}^{-2} \text{ s}^{-1}$), a purely leptonic emission scenario seems unlikely. Following [11] and assuming a typical Galactic magnetic field

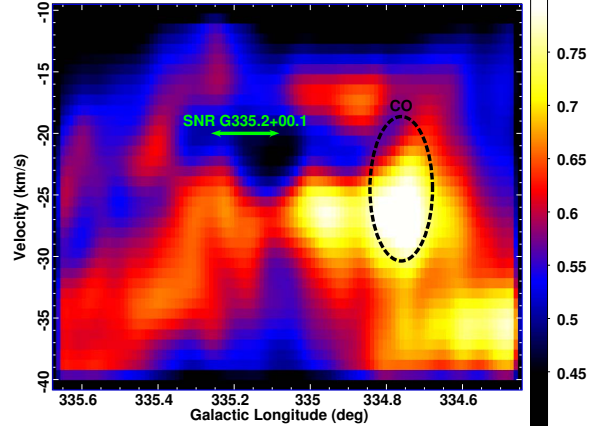


Figure 3: HI SGPS Galactic longitude–velocity plot (linear scale in K deg) integrated over the Galactic latitude range -0.11 to 0.24 deg . The position and extension of the ^{12}CO cloud is denoted by a dashed circle (black). The double arrow (green) shows the Galactic latitude and extension of SNR G335.2+00.1.

strength of $3 \times 10^{-6} \text{ G}$, and a photon index of $\Gamma = 2.2$ (as in the VHE domain), we estimate an integrated X-ray source flux of $\sim 1.1 \times 10^{-11} \text{ erg cm}^{-2} \text{ s}^{-1}$ (0.5–10.0 keV). This flux is a factor of ~ 25 more than what we measured from all but one point source which makes an identification of HESS J1626–490 with any of these sources unlikely. As the only sufficiently bright X-ray point source in the FoV can be identified with a triplet system of active main sequence stars it is most likely not related to HESS J1626–490. Furthermore, the upper limit for diffuse X-ray emission is a factor of ~ 2 lower than the expected value for HESS J1626–490 in a purely leptonic model.

Not detecting any X-ray source fulfilling the energetic requirements for a purely leptonic scenario favors a hadronic emission process such as dense clouds in the vicinity of a cosmic particle accelerator. Such a scenario will be discussed in the remaining part of this section. Dense molecular clouds are established VHE γ -ray emitters because they provide target material in regions of high cosmic-ray densities. Using data from the *Nanten* $^{12}\text{CO}(J=1-0)$ Galactic plane survey, we detected a molecular cloud that is morphologically consistent with HESS J1626–490. This object is located at a kinematic distance of $\sim 1.8 \text{ kpc}$. Following [12] (Eqs. 2 and 3), we estimated the required gas density to produce the observed VHE γ -ray signal ($F_{\gamma}(>0.6 \text{ TeV}) = 7.5 \times 10^{-12} \text{ ph cm}^{-2} \text{ s}^{-1}$ and $\Gamma = 2.2$) as $n \approx 10 \text{ cm}^{-3}$ assuming a cosmic-ray production efficiency of $\theta = 0.1$ and a distance of $d = 1.8 \text{ kpc}$. This value is an order of magnitude lower than the measured ^{12}CO mean density. Thus, this environment would be easily suited to providing the observed VHE γ -ray flux.

Now assuming that this ^{12}CO / HI cloud is indeed the source of the observed VHE γ -rays, a cosmic-ray accelerator would be needed in its vicinity. The nearby density depression seen in HI (see Sect. 3) might indicate the pres-

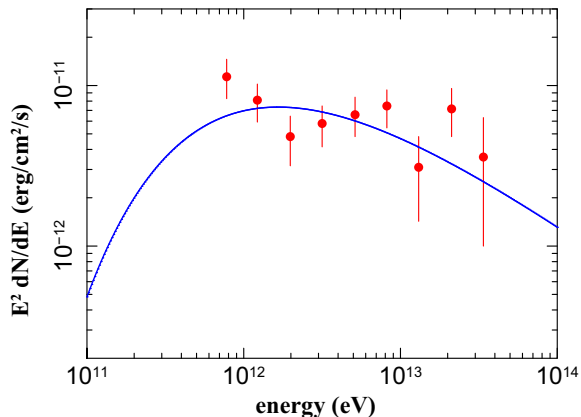


Figure 4: Spectral energy distribution of HESS J1626–490 showing the VHE γ -ray spectrum measured with H.E.S.S. (red). The solid line (blue) shows the hadronic model with the parameters that yield the best fit to the data ($R = 35$ pc, $t = 1.5 \times 10^5$ yr, $D_{10} = 9 \times 10^{25} \text{cm}^2 \text{s}^{-1}$).

ence of a recent catastrophic event, such as an SNR, giving rise to strong shocks that would have blown the neutral gas out. At $d = 1.8$ kpc the edge of this region would be at a distance of 8.1 pc from the $^{12}\text{CO}/\text{HI}$ cloud. It is striking that this HI feature is consistent in both position and angular extension with the SNR G335.2+00.1 [9]. Using the Σ -D relation the distance to SNR G335.2+00.1 was estimated as $d = 5$ kpc [13], which conflicts with the identification of SNR G335.2+00.1 with the HI depression seen at a distance of 1.8 kpc. However, the scatter in Σ -D distances for individual sources is quite large (see [14]) making a positive identification of SNR G335.2+00.1 and the HI depression seen at a kinematic distance of 1.8 kpc very well possible.

To explore the physical scenario of the interaction of the SNR G335.2+00.1 with the ^{12}CO molecular cloud in more detail, we adopted the model described by [15]. In this model hadronic cosmic rays with a powerlaw energy spectrum with index -2 and a total energy of 10^{50} erg are injected at the SNR shock into the ISM. The transport of these cosmic rays is described by an energy-dependent diffusion coefficient of the form $D_{\text{ISM}} = D_{10} \cdot E^{0.5}$, where E is the energy of the cosmic rays and D_{10} is the diffusion coefficient for an energy of 10 GeV. For the assumptions made by [15], the transport equation can be solved analytically and the expected γ -ray spectrum due to the production and subsequent decay of neutral pions can be calculated. Some of the model parameters can be constrained by the measurements presented in this work. These are the mass M , the density n of the molecular cloud and the distance d between the object and the observer. Also, a lower limit for the physical distance R between the SNR shock and the cloud was derived, which corresponds to the projected distance between these two objects (8.1 pc). However, it is still possible that the actual separation between SNR and cloud is in fact larger than this value due

to slightly different line-of-sight distances between these two objects and the observer. The remaining free model parameters are the age of the SNR t , the diffusion coefficient D_{10} and the radius R . Figure 4 shows the VHE γ -ray spectrum of HESS J1626–490 measured with H.E.S.S., together with the model with the parameters that yielded the best fit to the data ($R = 35$ pc, $t = 1.5 \times 10^5$ yr, $D_{10} = 9 \times 10^{25} \text{cm}^2 \text{s}^{-1}$). The best-fit value of D_{10} is about two orders of magnitude lower than the estimated mean value for the Galactic plane, however, it agrees well with comparable measurements of diffusion in the vicinity of other cosmic-ray accelerators (e.g., for the W28 region, see [16]). It has to be noted here, however, that the age t and the diffusion coefficient D_{10} are strongly correlated, and as t is not known for SNR G335.2+00.1 D_{10} is not very well constrained. Still the modeling shows that a hadronic scenario is indeed viable for HESS J1626–490 with reasonable physical parameters.

References

- [1] Aharonian, F., et al. *A&A*, **477** (2008): 353–363
- [2] Skrutskie, M. F., et al. *AJ*, **131** (2006): 1163–1183
- [3] Eger, P., et al. *A&A*, **526** (2011): A82+
- [4] Ebisawa, K., et al. *ApJ*, **635** (2005): 214–242
- [5] Mizuno, A., Fukui, Y. D. Clemens, R. Shah, & T. Brainerd, editor, *Milky Way Surveys: The Structure and Evolution of our Galaxy*, vol. 317 of *Astronomical Society of the Pacific Conference Series*. 2004 59–+
- [6] Brand, J., Blitz, L. *A&A*, **275** (1993): 67–+
- [7] Strong, A. W., et al. *A&A*, **422** (2004): L47–L50
- [8] Dickey, J. M., Lockman, F. J. *ARAA*, **28** (1990): 215–261
- [9] Green, D. A. *Bulletin of the Astronomical Society of India*, **37** (2009): 45–+
- [10] Reach, W. T., et al. *AJ*, **131** (2006): 1479–1500
- [11] Aharonian, F. A., Atoyan, A. M., Kifune, T. *MNRAS*, **291** (1997): 162–176
- [12] Aharonian, F. A., Drury, L. O., Voelk, H. J. *A&A*, **285** (1994): 645–647
- [13] Guseinov, O. H., Ankey, A., Tagieva, S. O. *Serbian Astronomical Journal*, **169** (2004): 65–+
- [14] Green, D. A. *Memorie della Societa Astronomica Italiana*, **76** (2005): 534–+
- [15] Gabici, S., Aharonian, F. A., Casanova, S. *MNRAS*, **396** (2009): 1629–1639
- [16] Gabici, S., et al. S. Boissier, M. Heydari-Malayeri, R. Samadi, & D. Valls-Gabaud, editor, *Proceedings of the Annual meeting of the French Society of Astronomy and Astrophysics*. 2010 313–+